Allometric Scaling and Seasonality in the Epidemics of Wildlife Diseases

Luca Bolzoni,[1,*] Andrew P. Dobson,[2,†] Marino Gatto,[3,‡] and Giulio A. De Leo[1,§]

1. Dipartimento di Scienze Ambientali, Università degli Studi di Parma, Viale Usberti 11/A, 43100 Parma, Italy;
2. Department of Ecology and Evolutionary Biology, Princeton University, Princeton, New Jersey 08544;
3. Dipartimento di Elettronica e Informazione, Politecnico di Milano, Via Ponzio 34/5, 20133 Milano, Italy

Submitted February 21, 2008; Accepted June 26, 2008; Electronically published October 23, 2008

Online enhancements: appendixes.

ABSTRACT: We present a susceptibles-exposed-infectives (SEI) model to analyze the effects of seasonality on epidemics, mainly of rabies, in a wide range of wildlife species. Model parameters are cast as simple allometric functions of host body size. Via nonlinear analysis, we investigate the dynamical behavior of the disease for different levels of seasonality in the transmission rate and for different values of the pathogen basic reproduction number (R_0) over a broad range of body sizes. While the unforced SEI model exhibits long-term epizootic cycles only for large values of R_0, the seasonal model exhibits multiyear periodicity for small values of R_0. The oscillation period predicted by the seasonal model is consistent with those observed in the field for different host species. These conclusions are not affected by alternative assumptions for the shape of seasonality or for the parameters that exhibit seasonal variations. However, the introduction of host immunity (which occurs for rabies in some species and is typical of many other wildlife diseases) significantly modifies the epidemic dynamics; in this case, multiyear cycling requires a large level of seasonal forcing. Our analysis suggests that the explicit inclusion of periodic forcing in models of wildlife disease may be crucial to correctly describe the epidemics of wildlife that live in strongly seasonal environments.

Keywords: epidemics model, wildlife disease, rabies, seasonality, allometry, bifurcation analysis.

* Corresponding author; e-mail: luca.bolzoni@nemo.unipr.it.

† E-mail: dobber@princeton.edu.

‡ E-mail: gatto@elet.polimi.it.

§ E-mail: giulio.deleo@unipr.it.

Am. Nat. 2008. Vol. 172, pp. 818–828.
0003-0147/2008/17206-50266$15.00.
DOI: 10.1086/593000

Seasonal forcing can have a dramatic impact on the dynamics of ecological and epidemiological nonlinear systems (Olsen et al. 1988; Hanski et al. 1993; Keeling et al. 2001). Realistic models of disease dynamics must undoubtedly account for the influence of seasonally varying exogenous factors (Olsen and Schaffer 1990; Greenman et al. 2004; Koelle et al. 2005*b*; Altizer et al. 2006). In fact, seasonal variations in host birth rate, social aggregation, and resource availability are central ecological features in all temperate and in many tropical habitats (Aron and Schwartz 1984; Altizer et al. 2006). Usually, wildlife birth rates peak in spring (e.g., see Bingham and Purchase 2002), while intraspecific competition increases in winter, when resources become scarce. Epidemiological parameters may also exhibit a seasonal trend; in particular, contact and transmission rates are inherently linked to animal mobility and social behavior. For example, the transmission of rabies among African black-backed jackals (*Canis mesomelas*) is facilitated by the dry season, when they increase their home range because of the scarcity of water (McKenzie 1993). Among European red foxes (*Vulpes vulpes*), the transmission coefficient of rabies increases with their mobility during the mating season and decreases when parents become more sedentary while they raise their offspring (Pastoret and Brochier 1999).

The effect of seasonality on host-parasite dynamics has received increasing attention in the past 20 years, especially in human diseases (Hethcote and York 1984; Bolker and Grenfell 1993; Grenfell et al. 1995; Kamo and Sasaki 2002; Greenman et al. 2004). Several studies have shown that seasonality in transmission rates can enormously complicate the population dynamics of host-parasite interaction and produce a variety of model behaviors. Technically, this corresponds to a sequence of model bifurcations that cycles with multiyear periods or even chaos for high levels of seasonal variation (Schwartz and Smith 1983; Aron and Schwartz 1984; Schwartz 1985; Keeling and Grenfell 1997; Keeling et al. 2001; Rohani et al. 2002; Greenman et al. 2004). This has recently led to new questions regarding

the adaptive dynamics of pathogens in a seasonal environment (Kamo and Sasaki 2005; Koelle et al. 2005*a*) and the maintenance of pathogen diversity (McKenzie et al. 2001).

The importance of seasonality in population ecology has long been recognized (Nisbet and Gurney 1982), but the role of seasonal fluctuations in wildlife diseases has attracted less attention than in human diseases, probably because of the general lack of extensive historical records of wildlife disease. As notable exceptions, Ruxton (1996) analyzed a susceptible, exposed but not infectious yet, infective, and recovered (SEIR) model of bovine tuberculosis in a badger host population capable of Malthusian growth and showed that seasonality in model parameters is unable to sustain epidemic cycles, and Briggs and Godfray (1996) studied the interaction between an insect and its pathogen in a seasonal environment when host dynamics are characterized by discrete generations.

On the other hand, the population dynamics of a free-living host are generally affected by intraspecific competition for resources or space. Although Ireland et al. (2004) have recently analyzed the complex dynamics of a seasonally forced susceptibles-infectives-recovered (SIR) model of a self-regulating population, a systematic analysis of a seasonally forced susceptibles-exposed-infectives (SEI) model of a self-regulating wildlife host has not been presented yet. The SIR framework does not account for the time delay between the onset of infection and the actual infectivity of the host. This delay is particularly important for understanding the dynamics of disease in wildlife, as pointed out by Anderson et al. (1981) in their seminal SEI model of rabies. In fact, if the latent period (the average time spent in the infected but not infectious class) is sufficiently long, the population dynamics of the nonseasonal host can be characterized by sustained oscillations (Swart 1989; Pugliese 1991). The interplay between the intrinsic tendency of these nonlinear epidemiological systems to oscillate with seasonal fluctuations of host fertility or transmission rate can elicit complex dynamical patterns (Keeling et al. 2001). This was anticipated by Kuznetsov and Piccardi (1994), who derived the general bifurcation diagram of a seasonally forced SEIR model of human diseases in a constant population.

The aim of this article is to thoroughly investigate the dynamics of seasonally forced SEI(R) models of lethal diseases in wildlife. We use an SEI model of rabies as a reference example because rabies is one of the most significant zoonoses worldwide and can affect a wide range of host species. Rabies dynamics can be well described by SEI models: the disease has a considerable latent period (usually longer than the infectious one) and assures low survival probability to the full-blown infected (absence of recovery class). On the other hand, in some species (such as raccoons and skunks), individuals exposed to rabies can develop natural immunity without developing the full-blown disease (i.e., without becoming infected). Moreover, the key features of its dynamics can be captured in a quite general mathematical framework that applies to other infectious diseases. As a consequence, the rabies SEI model provides important general insights into the dynamical properties of a wide range of zoonoses.

Rabies is a generalist and can infect hosts ranging in mass from a few grams (e.g., mice) to several hundreds of kilograms (e.g., bears). Thus, we perform the epidemiological analysis casting host demographic rates as allometric functions of host body size. In fact, larger hosts are expected to have longer life expectancies, smaller reproductive rates, slower dynamics, and sparser population densities compared with those of smaller host species (Peters 1983). Moreover, Bolzoni et al. (2008) showed that oscillations arising in the autonomous (i.e., nonseasonal) SEI model of a rabid host scale allometrically with body size. In particular, this work showed that hosts with larger body size exhibit longer periods of oscillation. Because fluctuations in the fertility and/or mortality of the host as well as in the transmission rate typically have a 1-year period, the interplay of seasonal forcing with the intrinsic oscillation frequency due to host-pathogen interaction may be different for hosts with different body sizes. Specifically, we assess here whether the introduction of seasonality can explain the observed patterns of multiyear periodicity in rabies epidemics. Also, we extend this analysis to diseases other than rabies by investigating the dynamics of a diseased host that is able to develop some level of immune response. Although this may be unlikely for rabies, it does often occur in other viral wildlife diseases such as distemper, brucellosis, and hog cholera.

This article is organized as follows: in the next section, we introduce the allometrically scaled SEI epidemic model originally developed by Anderson et al. (1981) and thoroughly described by Bolzoni et al. (2008). Then, we introduce seasonality, and using bifurcation analysis, we investigate the effect of different levels of seasonality in the transmission coefficient on the population dynamics of the infected host for species characterized by a wide range of body sizes. To verify the robustness of the results, we also derive the bifurcation diagrams when host birth rate (instead of transmission coefficient) exhibits seasonal fluctuations, and we investigate the effect of different shapes of seasonal forcing functions. We then modify the model to include an immune class and analyze the population dynamics under this new assumption.

The Seasonal SEI Model

The first SEI model of rabies was derived in the seminal article by Anderson et al. (1981) to describe the spread of

this infectious disease in European foxes and assess the efficacy of culling and vaccination for disease control and eradication. Some years later, Coyne et al. (1989) presented a modified version of the epidemiological model so as to account also for the development of acquired immunity in raccoons. In this work, we will use mainly the original version of Anderson et al.'s (1981) model (referred to as model [1]), which does not include an immune class, namely,

$$\frac{dS}{dt} = \nu S - (\mu + \gamma N)S - \beta SI, \tag{1a}$$

$$\frac{dE}{dt} = \beta SI - (\sigma + \mu + \gamma N)E, \tag{1b}$$

$$\frac{dI}{dt} = \sigma E - (\alpha + \mu + \gamma N)I. \tag{1c}$$

Here t is time (years); S, E, and I are the densities (no. individuals km^{-2}) of susceptible, infected but not infectious (exposed), and infective individuals in the population, respectively; N is the total population density, that is, $N = S + E + I$; ν, μ, and γ are the ecological parameters of the intrinsic birth rate, the intrinsic death rate, and the intraspecific competition coefficient, respectively; σ and α are the epidemiological parameters of the latency rate ($1/\sigma$ being the mean latency period) and disease-induced mortality, respectively; and β is the transmission coefficient. We refer to existing literature for a comprehensive stability analysis of the unforced SEI model (Swart 1989; Pugliese 1991; Gao et al. 1995).

Direct measurements of the transmission coefficient are difficult to obtain without extensive field data. In contrast, estimates of basic host demography and epidemiology are available for many species. Several comparative studies show that they scale with species weight as simple allometric relationships. Therefore, the aims of our analyses are to characterize the epidemiological regimes of rabies for a broad range of transmission coefficients and to predict threshold values of β for species encompassing a wide range of body sizes.

According to Silva and Downing (1995) and Cable et al. (2007) and following De Leo and Dobson (1996), we cast the demographic and epidemiological parameters of the model as allometric functions of mean host body size w (kg):

$$\nu = 1.0w^{-0.25}, \tag{2a}$$

$$\mu = 0.4w^{-0.25}, \tag{2b}$$

$$K = \frac{\nu - \mu}{\gamma} = 16.2w^{-0.70}, \tag{2c}$$

$$\sigma = 20w^{-0.25}, \tag{2d}$$

$$\alpha = 100w^{-0.25}, \tag{2e}$$

where K is carrying capacity (no. individuals km^{-2}) and the rates, as described previously, are given per year. Even though this model is quite simple, it is able to capture the main features of the population dynamics of rabies. A detailed analysis of the dynamics of the nonseasonal allometric SEI model of a lethal disease has been presented by Bolzoni et al. (2008). Our previous work shows that the threshold value of the transmission coefficient for the disease to establish in the population scales allometrically with host body size (exponent = 0.45), as well as the threshold value for limit cycles to occur. In contrast, the threshold value of the basic reproduction number $R_0 = \sigma\beta K/(\sigma + \nu)(\alpha + \nu)$ for sustained oscillations to occur is independent of host size.

To analyze the effect of seasonality on the basic SEI model, we assume that the transmission rate can be expressed as a sinusoidal function of time t (Dietz 1976),

$$\beta(t) = \beta_0[1 + \varepsilon \sin(2\pi t)], \tag{3}$$

where β_0 is the mean transmission coefficient (or baseline of transmission) and $0 \le \varepsilon \le 1$ is the degree of seasonality (or strength of the seasonal forcing). The periodically forced model is thus obtained by substituting equation (3) into model (1) with the allometric relationships (2). The model behavior has been studied through nonlinear analysis (Kuznetsov 1995). We find those values of the parameters at which the model regimes undergo qualitative changes (so-called bifurcations). Typically, there can be a switch from equilibria to cycles or from single to multiple attractors. Bifurcation analysis is performed by using numerical continuation methods implemented in the specialized software LOCBIF (Khibnik et al. 1993) and CONTENT (Kuznetsov 1998). The dynamical features of the seasonal model are illustrated in "Results."

Results

Because finding empirical estimates of transmission coefficients in wildlife diseases is difficult (see, e.g., Begon et al. 1999), it is essential to understand how the behavior of the SEI model changes under a wide range of values assigned to parameters ε and β_0 that fully describe disease transmission in a seasonal environment. Figure 1 shows

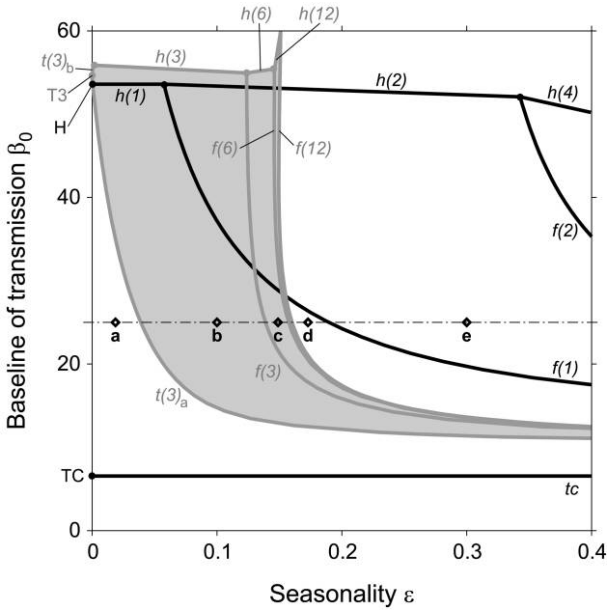

Figure 1: Bifurcation diagram of the seasonally forced SEI model in ε-β_0 parameter space for a host with body size $w = 1$ kg. The shaded area represents the parameter combinations for which model (1) displays multiyear epizootic cycles (with return time of 3 years between outbreaks). The population dynamics corresponding to the points *a*–*e* of the parameter space along the dash-dotted line are illustrated in figure 2. Labels are defined as follows (see app. A in the online edition of the *American Naturalist*): TC, transcritical bifurcation point; H, Hopf point; *tc*, transcritical bifurcation; $h(i)$, Neimark-Sacker bifurcations of cycle period i; $f(i)$, flip (period doubling) bifurcations of cycle period i; T3, 3-year epizootic cycle point; $t(3)_p$ tangent bifurcations.

the bifurcation diagram of the periodically forced SEI model in ε-β_0 space for a host with body mass of 1 kg. We show only bifurcation curves corresponding to attractors (stable equilibria and cycles) because this simplifies the interpretation of the diagram.

Along the vertical axis ($\varepsilon = 0$), it is possible to identify, for increasing values of the baseline of transmission β_0, the simple bifurcation sequence of the nonseasonal model. For $\beta_0 < \mathrm{TC}$ (where TC is the transcritical bifurcation point), the basic reproduction number R_0 is <1 (rabies cannot establish in the host population, and the system settles to its natural carrying capacity, a disease-free equilibrium). At TC, there is a so-called transcritical bifurcation characterized by $R_0 = 1$, the threshold for pathogen establishment. For $\mathrm{TC} < \beta_0 < \mathrm{H}$ (where H is the Hopf point), the pathogen can invade its host population, which eventually reaches a stable enzootic equilibrium. For $\beta_0 = \mathrm{H}$, the system undergoes a so-called Hopf bifurcation. For $\beta_0 > \mathrm{H}$, the disease model exhibits stable epizootic cycles; the period of oscillation is larger than 2 years and increases for increasing values of the transmission coefficient.

The introduction of seasonality ($\varepsilon > 0$) does not affect the threshold for the disease-free equilibrium, yet it remarkably changes the model behavior for $\beta_0 > \mathrm{TC}$. Quite obviously, a small degree of seasonality transforms the enzootic equilibrium of the nonseasonal, unforced model into an epizootic 1-year cycle (see fig. 2*A*). However, stron-

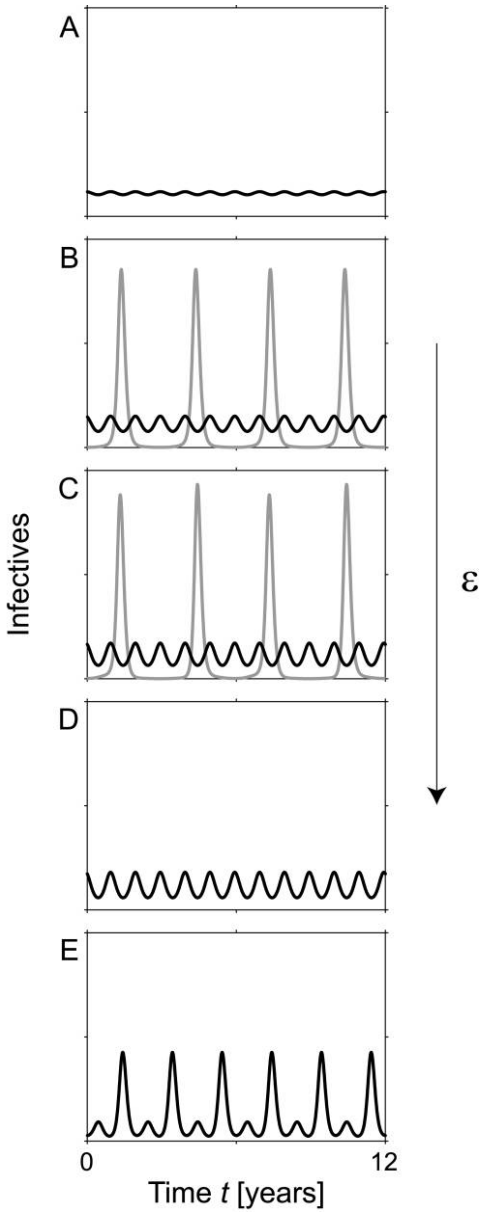

Figure 2: Time course of the infective hosts $I(t)$ in the attractors of the periodically forced SEI model. *A*–*E* are obtained by increasing the value of seasonality ε along the dash-dotted line in figure 1 (*a*–*e*). In *B* and *C*, there are two coexisting attractors (*black and gray curves*).

ger seasonal fluctuations of the transmission coefficient $\beta(t)$ can give rise to more complex dynamic behaviors corresponding to the bifurcation curve $f(1)$ and those regimes in the ε-β_0 plane that are mainly rooted in point T3 (the 3-year epizootic cycle point) on the β_0 axis.

Hereafter we report only major epidemiological results linked to the bifurcation analysis of model (1) and refer to appendix A in the online edition of the *American Naturalist* for a detailed description of figure 1. Along the curve $f(1)$, the 1-year cycle undergoes a so-called flip bifurcation. It changes to a period-2 cycle, a phenomenon called period doubling (see the time trajectory of fig. 2*E*, corresponding to *e* in fig. 1). More complicated is the explanation of the bifurcation curves rooted in T3. This is not a bifurcation point in the nonseasonal model ($\varepsilon = 0$); it is the value of the transmission coefficient corresponding to an epizootic 3-year cycle. According to the classical bifurcation theory of periodically forced models (Kuznetsov 1995), T3 is the root of a pair of so-called tangent bifurcation curves ($t(3)_a$ and $t(3)_b$ in fig. 1) that identify a region in the parameter space ε-β_0 in which population dynamics can resonate with the seasonal forcing function, a phenomenon called frequency locking. This gives rise to multiyear cycles with periods that are multiples of 3 years. As a consequence, within this region, two attractors coexist (fig. 1, *shaded area*): the first one corresponds to the small period-1 epizootic cycle generated by the seasonal forcing function for $\beta_0 > \mathrm{TC}$ (see the black time trajectory in fig. 2*B*, corresponding to *b* in fig. 1). The second attractor is the multiyear cycle due to frequency locking. It is characterized by an outbreak occurring every 3 years, followed by a long interepidemic phase. For sufficiently small values of seasonality, the multiyear attractor is a period-3 epizootic cycle (see the gray time trajectory in fig. 2*B*). For increasing levels of seasonality, along the boundary $f(3)$ of figure 1, the period-3 cycle undergoes a flip bifurcation and is transformed into a period-6 cycle. The period-6 epizootic cycle is also characterized by disease outbreaks every 3 years and coexists with a period-1 epizootic cycle (see fig. 2*C*, corresponding to *c* in fig. 1). A further increase of the level of seasonality produces a cascade of period-doubling bifurcations ($f(6)$, $f(12)$, …, $f(\infty)$) that occurs close to $f(3)$. Along $f(\infty)$, the multiyear cycle bifurcates into chaos, but numerical simulations from several initial conditions have shown that the basin of attraction of the chaotic attractor is too small to have any ecological and epidemiological significance. As a consequence, population dynamics basically converge toward attractors characterized by disease outbreaks every year (see fig. 2*D*, 2*E*, corresponding to *d* and *e* in fig. 1).

According to the bifurcation theory for seasonally forced models, along the vertical axis ($\varepsilon = 0$), there exist infinite points T4, T5, …, of frequency locking corresponding to cycles of period 4, 5, …, in which bifurcation curves similar to those originated in point T3 are rooted. We have omitted these curves in figure 1 because of their decreased ecological significance. In general, periodic solutions with large oscillation periods have very small basins of attraction (Schwartz 1985), and the state of the system in the presence of environmental noise is very likely to converge toward attractors with smaller oscillation periods (Greenman et al. 2004). In our case, the system converges to either the small, smooth, period-1 cycle or the cycles characterized by an outbreak occurring every 3 years.

Figure 3 provides a synoptic view of the dynamic behavior of host species characterized by three different body sizes: 1, 5, and 10 kg. To facilitate the comparative analysis, we have rescaled the vertical axis as a function of the average basic reproduction number because R_0 is proportional to the mean transmission coefficient β_0.

The bifurcation diagrams show that hosts with small body size (and large birth and death rates according to the allometric relationships) may exhibit dynamic regimes more complex than those of hosts with large body size (and small birth and death rates). As shown in figure 3*B*, 3*C*, the cascade of flip bifurcations involving period-1 cycles is not present in hosts of 5 and 10 kg. Moreover, multiyear cycles of larger hosts (feasible in shaded areas of fig. 3*B*, 3*C*) have larger periods (4 years) than cycles of 1-kg hosts. As a consequence, hosts with larger body size exhibit a longer interepidemic phase than hosts with smaller body size. In addition, hosts with large body size can exhibit multiyear epizootic cycles only for values of the basic reproduction number R_0 larger than those of hosts with small body size. Accordingly, for R_0 values ranging between 2 and 3, only small, not large, species can exhibit multiyear periodicity.

Numerical simulations of the seasonal SEI model dynamics, starting from different initial conditions, show that in parameter regions in which multiple attractors coexist (shaded areas in figs. 1, 3), the attractor with the lowest frequency-locking period (3 years for hosts of 1 kg, 4 years for hosts of 5 and 10 kg) has the largest basin of attraction. In the case of *b* in figure 1, for a host of 1 kg, simulations starting from initial conditions chosen in the range $0.75K < S_0 < K$ and $0 < I_0 < 0.01K$ show that the basin of the period-3 cycle is about twice as large as that of the period-1 cycle (62% of the trajectories converge to a period-3 cycle, 25% to a period-1 cycle, and 13% to epizootic cycles with periods larger than 3 years; see also fig. A1 in the online edition of the *American Naturalist*). As a consequence, numerical simulations confirm the theoretical prediction that dynamical regimes corresponding to the smallest frequency-locking period are the most likely to occur.

Figure 4 shows the smallest frequency-locking period as

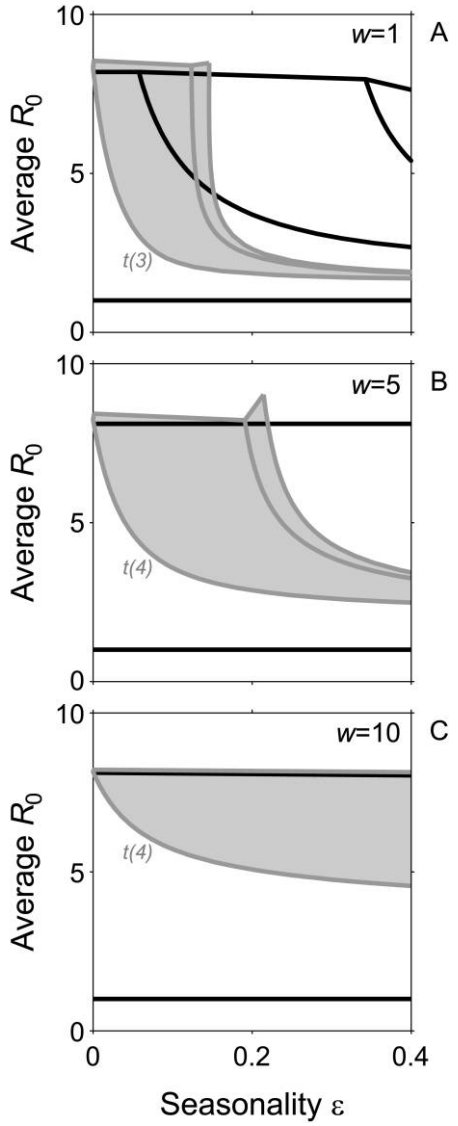

Figure 3: Effects of increasing host body size w on the bifurcation diagram of the seasonal SEI model in ε-R_0 space for (*A*) $w = 1$ kg (e.g., mustelids), (*B*) $w = 5$ kg (e.g., foxes), and (*C*) $w = 10$ kg (e.g., jackals). Shaded areas represent the parameter combinations for which model (1) displays multiyear epizootic cycles. The return time between epidemics is 3 years for hosts with $w = 1$ kg (*A*, *shaded area*) and 4 years for hosts with $w = 5$, 10 kg (*B*, *C*, *shaded areas*); $t(i)$, tangent bifurcations of cycle period i. Other parameters and curves are as defined in figure 1.

a function of the host body size (stepwise line) as predicted by the model. It also compares the prediction with the oscillation period observed for some mammal species that are known to be important reservoirs for rabies. Log-log regression shows significant positive correlation between the observed period of epizootic cycles and host body size (slope = 0.49, 95% confidence interval [CI]: 0.28–0.58, $R^2 = 0.85$, $n = 10$). Reduced major axis regression was used to calculate the slope, and CIs were estimated by bootstrapping (1,000 iterations). The shaded area of figure 4 corresponds to all the feasible cyclic solutions arising via frequency locking. Therefore, the oscillation periods predicted by our seasonally forced SEI model match the observed ones quite well. In the case of the black-backed jackal, the period of oscillation predicted by the model parameterized according to the vital rates as given by equations (2) for a 7.7-kg animal is larger than the one observed by Courtin et al. (2000; 4 years instead of 3). Further analyses show that if carrying capacity is only slightly larger than that predicted by equation (2c), the model will generate cycles of the observed length. We have not been able to find information on epizootic cycles in rabies-infected species with body size larger than 15 kg. This is, however, in agreement with the prediction of our model that hosts with large body size will exhibit epizootic oscillations only for very large (and possibly nonrealistic) values of the basic reproduction number R_0.

Other Kinds of Seasonality

Seasonality may obviously affect demographic or epidemiological parameters other than the transmission rate.

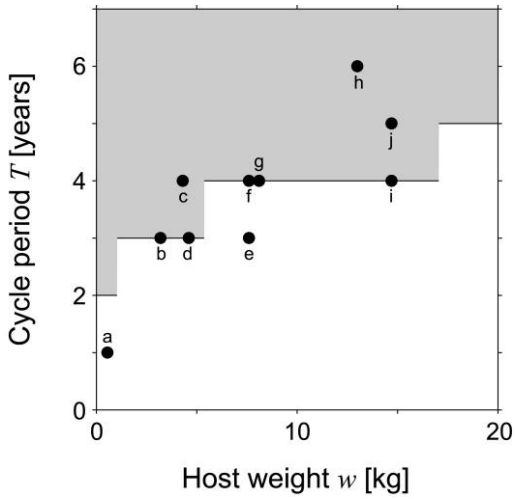

Figure 4: Comparison of minimum frequency-locking oscillation periods as predicted by seasonal SEI model against existing data for rabies epidemics in mammalian populations. The stepwise line represents the predicted period as a function of host body size w (kg). The points represent the minimum observed epizootic cycle period: *a*, mongoose; *b*, arctic fox; *c*, northern raccoon; *d*, red fox; *e*, *f*, black-backed jackal; *g*, raccoon dog; *h*, Eurasian badger; *i*, *j*, feral dog (see table 1 for data details). The shaded area corresponds to parameter combinations for which multiyear cycles can occur in the seasonal SEI model. Parameters σ and α are set to $24w^{-0.25}$ and $100w^{-0.25}$, respectively.

The host fertility rate, for instance, usually exhibits quite regular fluctuations in both temperate and tropical areas, in correspondence to the succession of dry and rainy or warm and cold seasons. We have thus analyzed the dynamical properties of the model assuming that the host birth rate is a sinusoidal function of time (as described in White et al. 1996; Ireland et al. 2004), namely,

$$\nu(t) = \nu_0 w^{-0.25}[1 + \varepsilon \sin(2\pi t)], \tag{4}$$

where $\nu_0 w^{-0.25}$ is the average value of the intrinsic birth rate and ε reflects the magnitude of seasonal variations, as in equation (3). As shown in figure 5, the bifurcation diagram of model (1) under the assumption of seasonal birth rate (4) and constant transmission rate, plotted in ε-ν_0 space, is similar to that of the SEI model, with seasonal transmission rate depicted in figure 1. As in figure 1, the shaded area represents those parameter combinations for which disease outbreaks with 3-year return time are feasible. Further analysis, not reported here, shows that even in the case of seasonal birth rate, multiyear periodicity for realistic values of R_0 and ε is possible only for hosts with smaller body size.

Because the reproductive season might be remarkably short (as pointed out in Roberts and Kao 1998), we have also derived the bifurcation diagram of the model using more pulselike functions for the host birth rate,

$$\nu(t) = \nu_0 w^{-0.25} \frac{[1 + \varepsilon \sin(2\pi t)]^z}{\int_0^1 [1 + \varepsilon \sin(2\pi t)]^z dt}, \tag{5}$$

where larger z's correspond to smaller pulse width. It turns out that even in these cases, the bifurcation diagrams of the modified seasonal SEI models (analyzed for $z \leq 6$) are not topologically different from that of the model with a sinusoidal transmission rate.

As observed by Altizer et al. (2006), the actual dynamics depend on which parameters are assumed to be seasonal and the shape and level of seasonality. Yet, further analyses not reported here show that the qualitative behavior of the seasonal SEI model does not depend on which demographic or epidemiological parameters actually characterize the seasonal fluctuations (also in the cases of several parameters with seasonal fluctuations and differences in the phase between them), a phenomenon that was observed in other seasonally forced population models (Gragnani and Rinaldi 1995). The results we have derived here are thus quite robust with respect to alternative hypotheses of the type of seasonality.

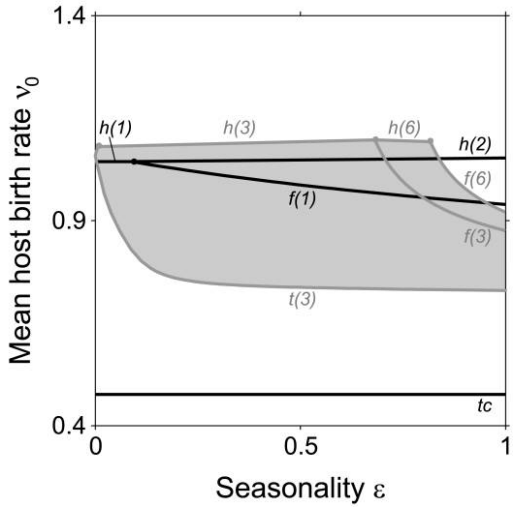

Figure 5: Bifurcation diagram for model (1) under the assumption of a seasonally fluctuating birth rate of the host (see eq. [5]) for hosts with body size $w = 1$ kg. The shaded area represents the parameter combinations for which model (1) displays multiyear epizootic cycles (return time of 3 years between outbreaks). Curves are as defined in figure 1. The mean transmission coefficient β_0 has been set to 50. Other parameter values are as defined in figure 1.

The Effect of the Host Immune Response

Most host species do not produce an effective immune response to the rabies virus, so the infection inexorably leads to the death of the infected individual. However, for a few wildlife species (such as raccoons and skunks), rabies occasionally may not be fatal (Coyne et al. 1989). More commonly, there is a large number of other diseases in which the host can develop temporary or permanent immunity. We explore the consequences of naturally acquired immunity of the host for the epidemic dynamics of the seasonally forced model. We incorporate a new class R into model (1) to account for recovered individuals that become immune as a result of infection. In the case of rabies, the exposed individuals become immune without developing a full-blown infection, that is, without moving from class E to class I. Hence, the epidemic model can be rewritten as follows:

$$\frac{dS}{dt} = \nu(S + R) - (\mu + \gamma N)S - \beta(t)SI, \tag{6a}$$

$$\frac{dE}{dt} = \beta(t)SI - (\sigma + \mu + \gamma N)E, \tag{6b}$$

$$\frac{dI}{dt} = (1 - \rho)\sigma E - (\alpha + \mu + \gamma N)I, \tag{6c}$$

$$\frac{dR}{dt} = \rho\sigma E - (\mu + \gamma N)R, \tag{6d}$$

where the *S*, *E*, and *I* classes have the same meaning as in model (1), as do parameters ν, μ, γ, σ, α, and $\beta(t)$. The parameter ρ represents the mean fraction of exposed individuals that develop a permanent immune response to the pathogen; *R* thus represents the density of recovered and immune hosts. We have assumed that immune individuals are fully reproductive. The total population density is *N*, namely, $N = S + E + I + R$. Obviously, when the probability of developing immunity tends to 0 ($\rho \to 0$), model (6) reduces to the classical SEI model (1). A similar nonseasonal version of model (6) was analyzed by Coyne et al. (1989) and Childs et al. (2000). They showed that even for small values of ρ, epizootic cycles cannot occur in the nonseasonal SEIR model. As a consequence, no multiyear epidemic cycles can arise through frequency locking in seasonally forced model (6). Figure 6 reports the bifurcation diagram of model (6) in ε-β_0 parameter space for two values of ρ. The shaded areas represent the parameter combinations for which disease outbreaks with 3-year return time are feasible for the SEIR model. We note that multiyear periodicity appears only in response to high levels of seasonal forcing and no longer occurs for low ε regardless of host body size. We refer to appendix B in the online edition of the *American Naturalist* for a detailed description of the bifurcation diagram depicted in figure 6.

Results obtained with model (6) are independent of the assumption, which holds for rabies, that exposed individuals skip full-blown infection before becoming immune. In fact, we have found similar results with an SEIR model in which exposed individuals become infected and infectious before developing immunity. It is interesting to note that results similar to those of our SEIR model with density dependence in the host demography were obtained by Kuznetsov and Piccardi (1994) for models of childhood diseases and by Casagrandi et al. (2006) for models of influenza epidemics in constant human populations. In both cases, host immunity was included.

Conclusions

In this work, we have analyzed the remarkable effects of seasonality in lethal diseases of self-regulating wildlife populations. Through allometric scaling of demographic and epidemiological parameters, we have examined the dynamics of the epidemiological system over a wide range of host body sizes. Our analysis shows that while the unforced SEI model exhibits multiyear epizootic cycles only for large values of the reproduction number R_0 (Bolzoni et al. 2008), the seasonally forced model can exhibit multiyear periodicity for much smaller and realistic values (<5) of R_0. Furthermore, bifurcation analysis shows that hosts with small mean body size may exhibit complex dynamics even with small levels of seasonal forcing. Resonance (frequency locking) is the key mechanism that determines the onset of multiyear periodic cycles for low transmission coefficients. Larger hosts have longer oscillation cycles, whose typical period can be predicted by our SEI model

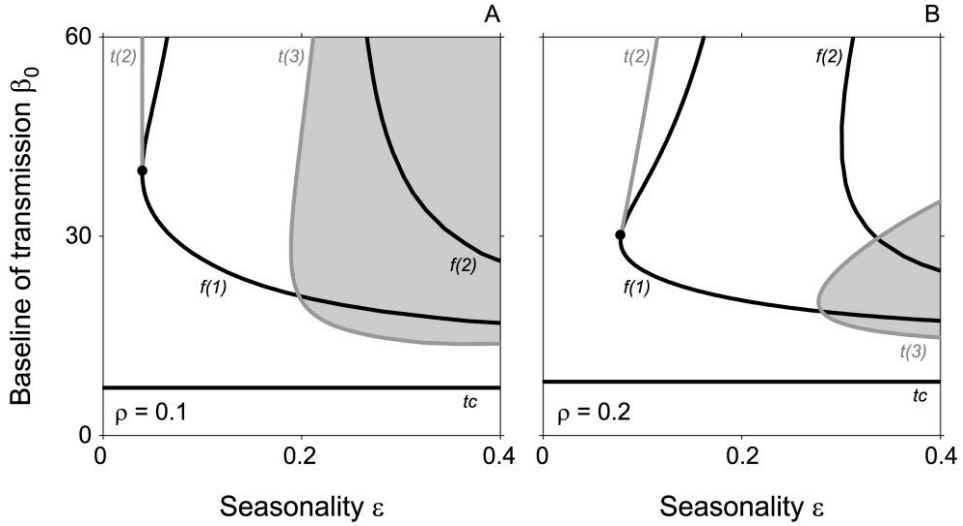

Figure 6: Bifurcation diagram in ε-β_0 space for SEIR model (6) with the coefficient of transmission periodically forced (see eq. [3]) for (*A*) $\rho = 0.1$ and (*B*) $\rho = 0.2$. Shaded areas represent the parameter combinations for which model (6) displays multiyear epizootic cycles (return time of 3 years between outbreaks). Note that epizootic cycles are feasible only for large values of seasonality. Other parameter values and curves are as defined in figure 1.

Table 1: Summary of data on rabies used in figure 4

Species name	Mass (kg)	Reference	Observed period (yr)	Reference	Predicted period (yr)
Mongoose *Herpestes javanicus*	.55	Carbone and Gittleman 2002	1	Everard et al. 1974	2
Arctic fox *Alopex lagopus*	3.19	Carbone and Gittleman 2002	3	Anderson et al. 1981	3
Northern raccoon *Procyon lotor*	4.3	Childs et al. 2000	4	Childs et al. 2000	3
Red fox *Vulpes vulpes*	4.6	Carbone and Gittleman 2002	3	Anderson et al. 1981	3
Black-backed jackal *Canis mesomelas*	7.7	Carbone et al. 2005	3	Courtin et al. 2000	4
Black-backed jackal *C. mesomelas*	7.7	Carbone et al. 2005	4	Walton and Joly 2003	4
Raccoon dog *Nyctereutes procyonides*	8.0	Atanasov 2005	4	Kim et al. 2006	4
Eurasian badger *Meles meles*	13.0	Carbone and Gittleman 2002	6	Smith 2002	4
Feral dog *Canis familiaris*	14.7	Butler et al. 2004	4	Bingham et al. 1999	4
Feral dog *C. familiaris*	14.7	Butler et al. 2004	5	Widdowson et al. 2002	4

Note: The observed period reports the minimum observed period of epizootic cycles; the predicted period shows the minimum frequency-locking period predicted by model (1).

for host species of different sizes. The prediction is in accordance with field observations on several mammals infected with rabies (see fig. 4; table 1). This relationship could thus be used to predict the outbreak frequency for newly established diseases by knowing the host body size only.

Our analysis shows that the explicit consideration of the latency period may dramatically change the population dynamics of the infectious disease with respect to what is predicted by susceptibles-infectives (SI)-like models of a self-regulating host population (Ireland et al. 2004). In fact, multiyear periodicity can occur even for very low levels of seasonality in the case of a seasonally forced SEI model, while this is not possible in the simpler SI-like models. Moreover, in the seasonally forced SEI model, high levels of seasonality coupled with high values of the basic reproduction number R_0 can potentially produce chaotic dynamics. However, the basins of attraction of the chaotic attractors are quite small, and even for intermediate or high levels of seasonality, the system basically tends to display yearly peaks of infectives (see fig. 2*D*, 2*E*).

These conclusions are quite robust with respect to alternative assumptions about how seasonality affects the model parameters. The same qualitative structure of the bifurcation diagram is retained when seasonality is included in demographic or epidemiological parameters other than transmission rate, even when more than one parameter has seasonal oscillation or when significant phase differences between oscillations of the seasonally forced parameters are included. Also, different shapes of the seasonal forcing function do not substantially alter the bifurcation diagram.

By contrast, if the disease causes an immune response with subsequent recovery (SEIR model), no multiyear periodicity occurs at low levels of seasonality, even when only a small fraction of infected hosts is able to develop such a response. Therefore, immunity has a crucial role in determining the dynamic regimes of wildlife diseases. This model behavior suggests that a correct estimate of the degree of immunity in the host population is necessary to predict the disease dynamics. This has important implications for implementing successful control policies. For instance, SEIR models can effectively describe the immunity induced in a host population by vaccination. Because vaccination policies increase the immunity ρ, they can drive host population dynamics from long-period epizootic cycles with large epidemic peaks to cycles with a short period for the same level of seasonality.

A number of processes that are not accounted for in this study might be relevant in determining the observed detailed patterns of specific rabies outbreaks. Spatial dynamics, multiple-strain interactions, and stochastic fade-out of the disease during the endemic phase (Mollison 1991; Mollison and Levin 1995; Rohani et al. 2002; Real et al. 2005) are obviously key factors that are considered important drivers of disease dynamics. Nevertheless, the allometric scaling approach adopted here provides key insights into the broad patterns of behavior likely to be observed in a large class of host species exposed to lethal pathogens and living in seasonal environments. In fact, as already outlined by Grenfell et al. (1995) and Keeling et al. (2001) for human disease, the explicit introduction of seasonality into models of host-parasite interaction in wildlife is a crucial element of realism. Without this key ingredient, it would be impossible to reproduce and ex-

plain the multiyear cycles observed for low values of the basic reproduction number.

Acknowledgments

We are very grateful to R. Casagrandi for his invaluable suggestions and remarks and to L. Real for his useful comments that improved the manuscript. This work was supported in part by the National Center for Ecological Analysis and Synthesis (a center funded by National Science Foundation [NSF] grant DEB-0072909 and the University of California at Santa Barbara, Seasonality and Infectious Diseases Group [to L.B. and G.A.D.L.]), NSF grant DEB-0225453 (to A.P.D.), and the Italian Ministry of Research project II04CE49G8 (to L.B., M.G., and G.A.D.L.).

Literature Cited

Altizer, S., A. P. Dobson, P. Hosseini, P. Hudson, M. Pascual, and P. Rohani. 2006. Seasonality and the dynamics of infectious diseases. Ecology Letters 9:467–484.

Anderson, R. M., H. C. Jackson, R. M. May, and A. M. Smith. 1981. Population dynamics of fox rabies in Europe. Nature 289:765–771.

Aron, J. L., and I. B. Schwartz. 1984. Seasonality and period-doubling bifurcations in an epidemic model. Journal of Theoretical Biology 110:665–679.

Atanasov, A. T. 2005. Allometric relationship between the length of pregnancy and body weight in mammals. Bulgarian Journal of Veterinary Medicine 8:13–22.

Begon, M., S. M. Hazel, D. Baxby, K. Bown, R. Cavanagh, J. Chantrey, T. Jones, and M. Bennett. 1999. Transmission dynamics of a zoonotic pathogen within and between wildlife host species. Proceedings of the Royal Society B: Biological Sciences 266:1939–1945.

Bingham, J., and G. K. Purchase. 2002. Reproduction in the jackals *Canis adustus* Sundevall, 1846, and *Canis mesomelas* Schreber, 1778 (Carnivora: Canidae), in Zimbabwe. African Zoology 37:21–26.

Bingham, J., C. M. Foggin, A. I. Wanderler, and F. W. G. Hill. 1999. The epidemiology of rabies in Zimbabwe. 1. Rabies in dogs (*Canis familiaris*). Onderstepoort Journal of Veterinary Research 66:1–10.

Bolker, B. M., and B. T. Grenfell. 1993. Chaos and biological complexity in measles dynamics. Proceedings of the Royal Society B: Biological Sciences 251:75–81.

Bolzoni, L., G. A. De Leo, M. Gatto, and A. P. Dobson. 2008. Body-size scaling in an SEI model of wildlife disease. Theoretical Population Biology 73:374–382.

Briggs, C. J., and H. C. J. Godfray. 1996. The dynamics of insect-pathogen interactions in seasonal environments. Theoretical Population Biology 50:149–177.

Butler, J. R. A., J. T. du Toit, and J. Bingham. 2004. Free-ranging domestic dogs (*Canis familiaris*) as predators and prey in rural Zimbabwe: threats of competition and disease to large wild carnivores. Biological Conservation 115:369–378.

Cable, J. M., B. J. Enquist, and M. E. Moses. 2007. The allometry of host-pathogen interactions. PLoS One 2:e1130.

Carbone, C., and J. Gittleman. 2002. A common rule for the scaling of carnivore density. Science 295:2273–2276.

Carbone, C., G. Cowlishaw, N. J. B. Isaac, and J. M. Rowcliffe. 2005. How far do animals go? determinants of day range in mammals. American Naturalist 165:290–297.

Casagrandi, R., L. Bolzoni, S. A. Levin, and V. Andreasen. 2006. The SIRC model and influenza A. Mathematical Biosciences 200:152–169.

Childs, J. E., A. T. Curns, M. E. Dey, L. A. Real, L. Feinstein, O. N. Bjørnstad, and J. W. Krebs. 2000. Predicting the local dynamics of epizootic rabies among raccoons in the United States. Proceedings of the National Academy of Sciences of the USA 97: 13666–13671.

Courtin, F., T. E. Carpenter, R. D. Paskin, and B. B. Chomel. 2000. Temporal patterns of domestic and wildlife rabies in central Namibia stock-ranching area, 1986–1996. Preventive Veterinary Medicine 43:13–28.

Coyne, M. J., G. Smith, and F. E. McAllister. 1989. Mathematical model for the population biology of rabies in raccoons in the mid-Atlantic states. American Journal of Veterinary Research 50:2148–2154.

De Leo, G. A., and A. P. Dobson. 1996. Allometry and simple epidemic models for microparasites. Nature 379:720–722.

Dietz, K. 1976. The incidence of infectious diseases under the influence of seasonal fluctuations. Lecture Notes in Biomathematics 11:1–15.

Everard, C. O. R., G. M. Baer, and A. James. 1974. Epidemiology of mongoose rabies in Grenada. Journal of Wildlife Diseases 10:190–196.

Gao, L. Q., J. Mena-Lorca, and H. W. Hethcote. 1995. Four SEI endemic models with periodicity and separatrices. Mathematical Biosciences 128:157–184.

Gragnani, A., and S. Rinaldi. 1995. A universal bifurcation diagram for seasonally perturbed predator-prey models. Bulletin of Mathematical Biology 57:701–712.

Greenman, J., M. Kamo, and M. Boots. 2004. External forcing of ecological and epidemiological systems: a resonance approach. Physica D 190:136–151.

Grenfell, B. T., B. M. Bolker, and A. Kleczkowski. 1995. Seasonality and extinction in chaotic metapopulations. Proceedings of the Royal Society B: Biological Sciences 259:97–103.

Hanski, I., P. Turchin, E. Korpimäki, and H. Henttonen. 1993. Population oscillations of boreal rodents: regulation by mustelid predators leads to chaos. Nature 364:232–235.

Hethcote, H. W., and J. A. York. 1984. Gonorrhea transmission dynamics and control. Springer, Berlin.

Ireland, J. M., R. A. Norman, and J. V. Greenman. 2004. The effect of seasonal host birth rates on population dynamics: the importance of resonance. Journal of Theoretical Biology 231:229–238.

Kamo, M., and A. Sasaki. 2002. The effect of cross-immunity and seasonal forcing in a multi-strain epidemic model. Physica D 165: 228–241.

———. 2005. Evolution toward multi-year periodicity in epidemics. Ecology Letters 8:378–385.

Keeling, M. J., and B. T. Grenfell. 1997. Disease extinction and community size: modeling the persistence of measles. Science 275:65–67.

Keeling, M. J., P. Rohani, and B. T. Grenfell. 2001. Seasonally forced dynamics explored as switching between attractors. Physica D 148: 335–347.

Khibnik, A. I., Y. A. Kuznetsov, V. V. Levitin, and E. V. Nikolaev. 1993. Continuation techniques and interactive software for bifurcation analysis of ODEs and iterated maps. Physica D 62:360–371.

Kim, C.-H., C.-G. Lee, H. C. Yoon, H.-M. Nam, C.-K. Park, J.-C. Lee, M.-I. Kang, and S.-H. Wee. 2006. Rabies, an emerging disease in Korea. Journal of Veterinary Medicine B 53:111–115.

Koelle, K., M. Pascual, and M. Yunus. 2005*a*. Pathogen adaptation to seasonal forcing and climate change. Proceedings of the Royal Society B: Biological Sciences 272:971–977.

Koelle, K., X. Rodò, M. Pascual, M. Yunus, and G. Mostafa. 2005*b*. Refractory periods and climate forcing in cholera dynamics. Nature 436:696–700.

Kuznetsov, Y. A. 1995. Elements of applied bifurcation theory. Springer, New York.

———. 1998. CONTENT: integrated environment for analysis of dynamical systems. Rapport de Recherche UPMA-98-224. École Normale Supérieure de Lyon, Lyon.

Kuznetsov, Y. A., and C. Piccardi. 1994. Bifurcation analysis of periodic SEIR and SIR epidemic models. Journal of Mathematical Biology 32:109–121.

McKenzie, A. A. 1993. Biology of the black-backed jackal with reference of rabies. Onderstepoort Journal of Veterinary Research 60: 367–371.

McKenzie, F. E., G. F. Killen, J. C. Beier, and W. H. Bossert. 2001. Seasonality, parasite diversity, and local extinctions in *Plasmodium falciparum* malaria. Ecology 82:2673–2681.

Mollison, D. 1991. Dependence of epidemic and population processes on basic parameters. Mathematical Biosciences 107:255–287.

Mollison, D., and S. Levin. 1995. Spatial dynamics of parasitism. Pages 384–398 *in* A. Dobson and B. Grenfell, eds. Ecology of infectious diseases in natural populations. Cambridge University Press, Cambridge.

Nisbet, R., and W. Gurney. 1982. Modelling fluctuating populations. Wiley, New York.

Olsen, L. F., and W. M. Schaffer. 1990. Chaos vs. noisy periodicity: alternative hypotheses for childhood epidemics. Science 249:499–504.

Olsen, L. F., G. L. Truty, and W. M. Schaffer. 1988. Oscillations and chaos in epidemics: a nonlinear dynamic study of six childhood diseases in Copenhagen, Denmark. Theoretical Population Biology 33:344–370.

Pastoret, P. P., and B. Brochier. 1999. Epidemiology and control of fox rabies in Europe. Vaccine 17:1750–1754.

Peters, R. H. 1983. The ecological implications of body size. Cambridge University Press, Cambridge.

Pugliese, A. 1991. An SEI epidemic model with varying population size. Pages 121–138 *in* S. Busenberg and M. Martelli, eds. Differential equation models in biology, epidemiology and ecology. Springer, New York.

Real, L. A., C. Russell, L. Waller, D. Smith, and J. Childs. 2005. Spatial dynamics and molecular ecology of North American rabies. Journal of Heredity 96:1–8.

Roberts, M. G., and R. R. Kao. 1998. The dynamics of an infectious disease in a population with birth pulses. Mathematical Biosciences 149:23–36.

Rohani, P., M. J. Keeling, and B. T. Grenfell. 2002. The interplay between determinism and stochasticity in childhood diseases. American Naturalist 159:469–481.

Ruxton, G. D. 1996. The effects of stochasticity and seasonality on model dynamics: bovine tuberculosis in badgers. Journal of Animal Ecology 65:495–500.

Schwartz, I. B. 1985. Multiple stable recurrent outbreaks and predictability in seasonally forced nonlinear epidemic models. Journal of Mathematical Biology 21:347–361.

Schwartz, I. B., and L. H. Smith. 1983. Infinite subharmonic bifurcation in a SEIR epidemic model. Journal of Mathematical Biology 18:233–253.

Silva, M., and J. A. Downing. 1995. The allometric scaling of density and body mass: a nonlinear relationship for terrestrial mammals. American Naturalist 145:704–727.

Smith, G. C. 2002. The role of the badger (*Meles meles*) in rabies epizootiology and the implications for Great Britain. Mammal Review 32:12–25.

Swart, J. H. 1989. Hopf bifurcation and stable limit cycle behavior in the spread of infectious diseases, with special application to fox rabies. Mathematical Biosciences 95:199–207.

Walton, L. R., and D. O. Joly. 2003. *Canis mesomelas*. Mammal Species 715:1–9.

White, K. A. J., B. T. Grenfell, R. J. Hendry, O. Lejeune, and J. D. Murray. 1996. Effect of seasonal host reproduction on host-macroparasite. Mathematical Biosciences 137:79–99.

Widdowson, M.-A., G. J. Morales, S. Chavez, and J. McGrane. 2002. Epidemiology of urban canine rabies, Santa Cruz, Bolivia, 1972–1997. Epidemiology and Infection 8:458–461.

Associate Editor: Tim Coulson
Editor: Donald L. DeAngelis